

Distributed Methods for High-dimensional and Large-scale Tensor Factorization

Kijung Shin

Dept. of Computer Science and Engineering
Seoul National University
Seoul, Republic of Korea
koreaskj@snu.ac.kr

U Kang

Dept. of Computer Science
KAIST
Daejeon, Republic of Korea
ukang@cs.kaist.ac.kr

Abstract—Given a high-dimensional and large-scale tensor, how can we decompose it into latent factors? Can we process it on commodity computers with limited memory? These questions are closely related to recommendation systems exploiting context information such as time and location. They require tensor factorization methods scalable with both the dimension and size of a tensor. In this paper, we propose two distributed tensor factorization methods, SALS and CDTF. Both methods are scalable with all aspects of data, and they show an interesting trade-off between convergence speed and memory requirements. SALS updates a subset of the columns of a factor matrix at a time, and CDTF, a special case of SALS, updates one column at a time. On our experiment, only our methods factorize a 5-dimensional tensor with 1B observable entries, 10M mode length, and 1K rank, while all other state-of-the-art methods fail. Moreover, our methods require several orders of magnitude less memory than the competitors. We implement our methods on MAPREDUCE with two widely applicable optimization techniques: local disk caching and greedy row assignment.

Keywords—Tensor factorization; Recommender system; Distributed computing; MapReduce

I. INTRODUCTION AND RELATED WORK

The recommendation problem can be viewed as completing a partially observable user-item matrix whose entries are ratings. Matrix factorization (MF), which decomposes the input matrix into a user factor matrix and an item factor matrix so that their multiplication approximates the input matrix, is one of the most widely used methods [2], [7], [14]. To handle web-scale data, efforts have been made to find distributed ways for MF, including ALS [14], DSGD [4], and CCD++ [12].

On the other hand, there have been attempts to improve the accuracy of recommendation by using additional information such as time and location. A straightforward way to utilize such extra factors is to model rating data as a partially observable tensor where additional dimensions correspond to the extra factors. As in the matrix case, tensor factorization (TF), which decomposes the input tensor into multiple factor matrices and a core tensor, has been used [5], [9], [13].

As the dimension of web-scale recommendation problems increases, a necessity for TF algorithms scalable with the dimension as well as the size of data has arisen. A promising way to find such algorithms is to extend distributed MF

Table I: Summary of scalability results. The factors which each method is scalable with are checked. Our proposed SALS and CDTF are the only methods scalable with all the factors.

	CDTF	SALS	ALS	PSGD	FLEXIFACT
Dimension	✓	✓	✓	✓	
Observations	✓	✓	✓	✓	✓
Mode Length	✓	✓			✓
Rank	✓	✓			✓
Machines	✓	✓	✓		

algorithms to higher dimensions. However, the scalability of existing methods including ALS [14], PSGD [8], and FLEXIFACT [1] is limited as summarized in Table I.

In this paper, we propose SALS and CDTF, distributed tensor factorization methods scalable with all aspects of data. SALS updates a subset of the columns of a factor matrix at a time, and CDTF, a special case of SALS, updates one column at a time. Our methods have distinct advantages: SALS converges faster, and CDTF is more memory-efficient. They can also be applied to any application handling large-scale and partially observable tensors, including social network analysis [3] and Web search [11].

The main contributions of our study are as follows:

- **Algorithm.** We propose two tensor factorization algorithms: SALS and CDTF. Their distributed versions are the only methods scalable with all the following factors: the dimension and size of data; the number of parameters; and the number of machines (Table I).
- **Analysis.** We analyze our methods and the competitors in a general N-dimensional setting in the following aspects: computational complexity, communication complexity, memory requirements, and convergence speed (Table II).
- **Optimization.** We implement our methods on MAPREDUCE with two novel optimization techniques: local disk caching and greedy row assignment. They speed up not only our methods (up to 98.2×) but also their competitors (up to 5.9×) (Figure 6).
- **Experiment.** We empirically confirm the superior scalability of our methods and their several orders of magnitude less memory requirements than their competitors. Only our methods analyze a 5-dimensional

Table II: Summary of distributed tensor factorization algorithms. The performance bottlenecks which prevent each algorithm from handling web-scale data are colored red. Only our proposed SALS and CDTF have no bottleneck. Communication complexity is measured by the number of parameters that each machine exchanges with the others. For simplicity, we assume that workload of each algorithm is equally distributed across machines, that the length of every mode is equal to I , and that T_{in} of SALS and CDTF is set to one.

Algorithm	Computational complexity (per iteration)	Communication complexity (per iteration)	Memory requirements	Convergence speed
CDTF	$O(\Omega N^2K/M)$	$O(NIK)$	$O(NI)$	Fast
SALS	$O(\Omega NK(N+C)/M + NIKC^2/M)$	$O(NIK)$	$O(NIC)$	Fastest
ALS [14]	$O(\Omega NK(N+K)/M + NIK^3/M)$	$O(NIK)$	$O(NIK)$	Fastest
PSGD [8]	$O(\Omega NK/M)$	$O(NIK)$	$O(NIK)$	Slow
FLEXIFACT [1]	$O(\Omega NK/M)$	$O(M^{N-2}NIK)$	$O(NIK/M)$	Fast

Table III: Table of symbols.

Symbol	Definition
\mathcal{X}	input tensor ($\in \mathbb{R}^{I_1 \times I_2 \times \dots \times I_N}$)
$x_{i_1 \dots i_N}$	(i_1, \dots, i_N) th entry of \mathcal{X}
N	dimension of \mathcal{X}
I_n	length of the n th mode of \mathcal{X}
$\mathbf{A}^{(n)}$	n th factor matrix ($\in \mathbb{R}^{I_n \times K}$)
$a_{i_n k}^{(n)}$	(i_n, k) th entry of $\mathbf{A}^{(n)}$
K	rank of \mathcal{X}
Ω	set of indices of observable entries of \mathcal{X}
$\Omega_{i_n}^{(n)}$	subset of Ω whose n th mode's index is equal to i_n
mS_n	set of rows of $\mathbf{A}^{(n)}$ assigned to machine m
\mathcal{R}	residual tensor ($\in \mathbb{R}^{I_1 \times I_2 \times \dots \times I_N}$)
$r_{i_1 \dots i_N}$	(i_1, \dots, i_N) th entry of \mathcal{R}
M	number of machines (reducers on MAPREDUCE)
T_{out}	number of outer iterations
T_{in}	number of inner iterations
λ	regularization parameter
C	number of parameters updated at a time
η_0	initial learning rate

tensor with 1B observable entries, 10M mode length, and 1K rank, while all others fail (Figure 4(a)).

The binary codes of our methods and several datasets are available at <http://kdm.kaist.ac.kr/sals>. The rest of this paper is organized as follows. Section II presents preliminaries for tensor factorization. Section III describes our proposed SALS and CDTF. Section IV presents the optimization techniques for them on MAPREDUCE. After providing experimental results in Section V, we conclude in Section VI.

II. PRELIMINARIES: TENSOR FACTORIZATION

In this section, we describe the preliminaries of tensor factorization and its distributed algorithms.

A. Tensor and the Notations

A tensor is a multi-dimensional array which generalizes a vector (1-dimensional tensor) and a matrix (2-dimensional tensor) to higher dimensions. Like rows and columns in a matrix, an N -dimensional tensor has N modes whose lengths are I_1 through I_N , respectively. We denote tensors with variable dimension N by boldface Euler script letters, e.g., \mathcal{X} . Matrices and vectors are denoted by boldface capitals, e.g., \mathbf{A} , and boldface lowercases, e.g., \mathbf{a} , respectively. We denote the entry of a tensor by the symbolic name of the tensor with its indices in subscript. For example, the (i_1, i_2) th entry of \mathbf{A} is denoted by $a_{i_1 i_2}$, and the (i_1, \dots, i_N) th entry of \mathcal{X} is denoted by $x_{i_1 \dots i_N}$. The i_1 th

row of \mathbf{A} is denoted by \mathbf{a}_{i_1*} , and the i_2 th column of \mathbf{A} is denoted by \mathbf{a}_{*i_2} . Table III lists the symbols used in this paper.

B. Tensor Factorization

There are several ways to define tensor factorization, and our definition is based on PARAFAC decomposition, which is one of the most popular decomposition methods, and nonzero squared loss with L2 regularization, whose weighted form has been successfully used in many recommendation systems [2], [7], [14]. Details about PARAFAC decomposition can be found in [6].

Definition 1 (Tensor Factorization):

Given an N -dimensional tensor $\mathcal{X} (\in \mathbb{R}^{I_1 \times I_2 \times \dots \times I_N})$ with observable entries $\{x_{i_1 \dots i_N} | (i_1, \dots, i_N) \in \Omega\}$, the rank K factorization of \mathcal{X} is to find factor matrices $\{\mathbf{A}^{(n)} \in \mathbb{R}^{I_n \times K} | 1 \leq n \leq N\}$ which minimize the following loss function:

$$L(\mathbf{A}^{(1)}, \dots, \mathbf{A}^{(N)}) = \sum_{(i_1, \dots, i_N) \in \Omega} \left(x_{i_1 \dots i_N} - \sum_{k=1}^K \prod_{n=1}^N a_{i_n k}^{(n)} \right)^2 + \lambda \sum_{n=1}^N \|\mathbf{A}^{(n)}\|_F^2. \quad (1)$$

Note that the loss function depends only on the observable entries. Each factor matrix $\mathbf{A}^{(n)}$ corresponds to the latent feature vectors of n th mode instances, and $\sum_{k=1}^K \prod_{n=1}^N a_{i_n k}^{(n)}$ corresponds to the interaction between the features.

C. Distributed Methods for Tensor Factorization

In this section, we introduce several tensor factorization algorithms suitable for distributed environments. The performances of them are summarized in Table II.

1) *Alternating Least Square (ALS)*: ALS [14] updates factor matrices one by one while keeping all other matrices fixed. When all factor matrices except one are fixed, (1) becomes a quadratic problem which is analytically solvable. Due to the independence between rows, each factor matrix can be updated row by row. The update rule for the rows of $\mathbf{A}^{(n)}$ is as follows:

$$\begin{aligned} [a_{i_n 1}^{(n)}, \dots, a_{i_n K}^{(n)}]^T &\leftarrow \arg \min_{[a_{i_n 1}^{(n)}, \dots, a_{i_n K}^{(n)}]^T} L(\mathbf{A}^{(1)}, \dots, \mathbf{A}^{(N)}) \\ &= (\mathbf{B}_{i_n}^{(n)} + \lambda \mathbf{I}_K)^{-1} \mathbf{c}_{i_n}^{(n)} \end{aligned} \quad (2)$$

where the (k_1, k_2) entry of $\mathbf{B}_{i_n}^{(n)} (\in \mathbb{R}^{K \times K})$ is

$$\sum_{(i_1, \dots, i_N) \in \Omega_{i_n}^{(n)}} \left(\prod_{l \neq n} a_{i_l k_1}^{(l)} \prod_{l \neq n} a_{i_l k_2}^{(l)} \right),$$

the k th entry of $\mathbf{c}_{i_n}^{(n)} (\in \mathbb{R}^K)$ is

$$\sum_{(i_1, \dots, i_N) \in \Omega_{i_n}^{(n)}} \left(x_{i_1 \dots i_N} \prod_{l \neq n} a_{i_l k}^{(l)} \right),$$

and \mathbf{I}_K is a K by K identity matrix. $\Omega_{i_n}^{(n)}$ denotes the subset of Ω whose n th mode's index is equal to i_n .

The proof of this update rule is as follows:

Proof:

$$\begin{aligned} \frac{\partial L}{\partial a_{i_n k}^{(n)}} &= 0, \forall k, 1 \leq k \leq K \\ \Leftrightarrow \sum_{(i_1, \dots, i_N) \in \Omega_{i_n}^{(n)}} &\left(\left(\sum_{s=1}^K \prod_{l=1}^N a_{i_l s}^{(l)} - x_{i_1 \dots i_N} \right) \prod_{l \neq n} a_{i_l k}^{(l)} \right) + \lambda a_{i_n k}^{(n)} \\ &= 0, \forall k \\ \Leftrightarrow \sum_{(i_1, \dots, i_N) \in \Omega_{i_n}^{(n)}} &\left(\sum_{s=1}^K \left(a_{i_n s}^{(n)} \prod_{l \neq n} a_{i_l s}^{(l)} \right) \prod_{l \neq n} a_{i_l k}^{(l)} \right) + \lambda a_{i_n k}^{(n)} \\ &= \sum_{(i_1, \dots, i_N) \in \Omega_{i_n}^{(n)}} \left(x_{i_1 \dots i_N} \prod_{l \neq n} a_{i_l k}^{(l)} \right), \forall k \\ \Leftrightarrow (\mathbf{B}_{i_n}^{(n)} + \lambda \mathbf{I}_K) [a_{i_n 1}^{(n)}, \dots, a_{i_n K}^{(n)}]^T &= \mathbf{c}_{i_n}^{(n)} \quad \blacksquare \end{aligned}$$

Updating a row, $\mathbf{a}_{i_n*}^{(n)}$ for example, using (2) takes $O(|\Omega_{i_n}|K(N+K) + K^3)$, which consists of $O(|\Omega_{i_n}^{(n)}|NK)$ to calculate $\prod_{l \neq n} a_{i_l 1}^{(l)}$ through $\prod_{l \neq n} a_{i_l K}^{(l)}$ for all the entries in $|\Omega_{i_n}^{(n)}|$, $O(|\Omega_{i_n}^{(n)}|K^2)$ to build $\mathbf{B}_{i_n}^{(n)}$, $O(|\Omega_{i_n}^{(n)}|K)$ to build $\mathbf{c}_{i_n}^{(n)}$, and $O(K^3)$ to invert $\mathbf{B}_{i_n}^{(n)}$. Instead of calculating the inverse, Cholesky decomposition, which also takes $O(K^3)$, can be used. Thus, updating every row of all the factor matrices once, which corresponds to a full ALS iteration, takes $O(|\Omega|NK(N+K) + K^3 \sum_{n=1}^N I_n)$.

In distributed environments, updating each factor matrix can be parallelized without affecting the correctness of ALS by distributing the rows of the factor matrix across machines so that they can be updated simultaneously. The parameters updated by each machine are broadcasted to all other machines so that they can be used to update the next factor matrix. The number of parameters each machine exchanges (sends or receives) with the others is $O(KI_n)$ for each factor matrix $\mathbf{A}^{(n)}$ and $O(K \sum_{n=1}^N I_n)$ per iteration. The memory requirements of ALS cannot be distributed, however. Since the update rule (2) possibly depends on all the entries of all other factor matrices, every machine is required to load all the factor matrices into their memory. This high memory requirement of ALS, which requires $O(K \sum_{n=1}^N I_n)$ memory space per machine, has been noted as a bottleneck of the scalability of ALS even in matrix factorization [4], [12].

2) Parallelized Stochastic Gradient Descent (PSGD):

PSGD [8] is a distributed algorithm based on stochastic gradient descent (SGD). PSGD randomly divides the observable entries of \mathcal{X} into M machines, and each machine runs SGD

independently. The updated parameters are averaged after each iteration. For each observable entry $x_{i_1 \dots i_N}$, $a_{i_n k}^{(n)}$ for all n and k , whose number is NK , are updated simultaneously by the following rule :

$$a_{i_n k}^{(n)} \leftarrow a_{i_n k}^{(n)} - 2\eta \left(\frac{\lambda a_{i_n k}^{(n)}}{|\Omega_{i_n}^{(n)}|} - r_{i_1 \dots i_N} \left(\prod_{l \neq n} a_{i_l k}^{(l)} \right) \right) \quad (3)$$

where $r_{i_1 \dots i_N} = x_{i_1 \dots i_N} - \sum_{s=1}^K \prod_{l=1}^N a_{i_l s}^{(l)}$. It takes $O(NK)$ to calculate $r_{i_1 \dots i_N}$ and $\prod_{l=1}^N a_{i_l k}^{(l)}$ for all k . Once they are calculated, since $\prod_{l \neq n} a_{i_l k}^{(l)}$ can be calculated as $(\prod_{l=1}^N a_{i_l k}^{(l)}) / a_{i_n k}^{(n)}$, calculating (3) takes $O(1)$, and thus updating all the NK parameters takes $O(NK)$. If we assume that \mathcal{X} entries are equally distributed across machines so that the number of \mathcal{X} entries assigned to each machine is $O(|\Omega|/M)$, the computational complexity per iteration is $O(NK|\Omega|/M)$. Averaging parameters can also be distributed, which incurs $O(K \sum_{n=1}^N I_n)$ parameter exchanges per machine. Like ALS, the memory requirements of PSGD cannot be distributed, and all the machines are required to load all the factor matrices into their memory, which requires $O(K \sum_{n=1}^N I_n)$ memory space per machine. Moreover, PSGD tends to converge slowly due to the non-identifiability of (1) [4].

3) *Flexible Factorization of Coupled Tensors (Flexi-FaCT)*: FLEXIFACT [1] is another SGD-based algorithm which generalizes matrix factorization algorithm DSGD [4] to higher dimensions. FLEXIFACT avoids the high memory requirement and slow convergence of PSGD [1], [4]. FLEXIFACT divides \mathcal{X} into M^N blocks, and M disjoint blocks that do not share common fibers (rows in a general n th mode) compose a stratum. FLEXIFACT processes \mathcal{X} stratum by stratum. For each stratum, the M blocks composing it are distributed across machines and processed independently. The update rule is the same as (3), and the computational complexity per iteration is $O(|\Omega|NK/M)$ as in PSGD. However, contrary to PSGD, averaging is not necessary because the sets of parameters updated by the machines are disjoint. In addition, the memory requirements of FLEXIFACT are distributed among the machines. Each machine only needs to load the parameters related to the block it processes, whose number is $(K \sum_{n=1}^N I_n)/M$, into its memory at a time. FLEXIFACT suffers from high communication cost, however. After processing one stratum, each machine sends the updated parameters to the machine which updates them in the next stratum. The number of parameters exchanged by each machine is at most $(K \sum_{n=2}^N I_n)/M$ per stratum and $M^{N-2} K \sum_{n=2}^N I_n$, where M^{N-1} is the number of strata, per iteration. Accordingly, the communication cost of FLEXIFACT increases exponentially with the dimension of \mathcal{X} and polynomially with the number of machines.

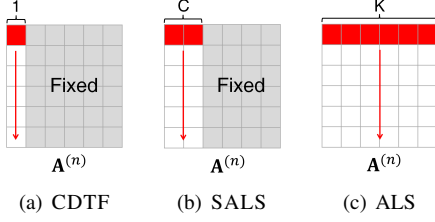


Figure 1: Update rules of CDTF, SALS, and ALS. CDTF updates each column of factor matrices entry by entry, SALS updates each C ($1 \leq C \leq K$) columns row by row, and ALS updates each K columns row by row.

Algorithm 1: Serial version of SALS

Input : \mathcal{X}, K, λ
Output: $\mathbf{A}^{(n)}$ for all n

```

1 initialize  $\mathcal{R}$  and  $\mathbf{A}^{(n)}$  for all  $n$ 
2 for outer iter = 1.. $T_{out}$  do
3   for split iter = 1.. $\lceil \frac{K}{C} \rceil$  do
4     choose  $k_1, \dots, k_C$  (from columns not updated yet)
5     compute  $\hat{\mathcal{R}}$ 
6     for inner iter = 1.. $T_{in}$  do
7       for  $n = 1..N$  do
8         for  $i_n = 1..I_n$  do
9           update  $a_{i_n k_1}^{(n)}, \dots, a_{i_n k_C}^{(n)}$  using (4)
10      update  $\mathcal{R}$  using (5)

```

III. PROPOSED METHODS

In this section, we propose subset alternating least square (SALS) and coordinate descent for tensor factorization (CDTF). They are scalable algorithms for tensor factorization, which is essentially an optimization problem whose loss function is (1) and parameters are the entries of factor matrices, $\mathbf{A}^{(1)}$ through $\mathbf{A}^{(N)}$. Figure 1 depicts the difference among CDTF, SALS, and ALS. Unlike ALS, which updates each K columns of factor matrices row by row, SALS updates each C ($1 \leq C \leq K$) columns row by row, and CDTF updates each column entry by entry. CDTF can be seen as an extension of CCD++ [12] to higher dimensions. Since SALS contains CDTF ($C = 1$) as well as ALS ($T_{in} = 1, C = K$) as a special case, we focus on SALS and additionally explain optimization schemes for CDTF.

A. Update Rule and Update Sequence

Algorithm 1 describes the procedure of SALS. \mathcal{R} denotes the residual tensor where $r_{i_1 \dots i_N} = x_{i_1 \dots i_N} - \sum_{k=1}^K \prod_{n=1}^N a_{i_n k}^{(n)}$. We initialize the entries of $\mathbf{A}^{(1)}$ to zeros and those of all other factor matrices to random values so that the initial value of \mathcal{R} is equal to \mathcal{X} (line 1). In every iteration (line 1), SALS repeats choosing C columns, k_1 through k_C , randomly without replacement (line 1) and updating them while keeping the other columns fixed, which is equivalent to the rank C factorization of $\hat{\mathcal{R}}$ where $\hat{r}_{i_1 \dots i_N} = r_{i_1 \dots i_N} + \sum_{c=1}^C \prod_{n=1}^N a_{i_n k_c}^{(n)}$. Once $\hat{\mathcal{R}}$ is computed (line 1), updating C columns of factor matrices matrix by matrix (line 1) is repeated T_{in} times (line 1). For each

factor matrix, since its rows are independent of each other in minimizing (1) when the other factor matrices are fixed, the entries are updated row by row (line 1) as follows:

$$[a_{i_n k_1}^{(n)}, \dots, a_{i_n k_C}^{(n)}]^T \leftarrow \arg \min_{[a_{i_n k_1}^{(n)}, \dots, a_{i_n k_C}^{(n)}]^T} L(\mathbf{A}^{(1)}, \dots, \mathbf{A}^{(N)}) \\ = (\mathbf{B}_{i_n}^{(n)} + \lambda \mathbf{I}_C)^{-1} \mathbf{c}_{i_n}^{(n)}, \quad (4)$$

where the (c_1, c_2) th entry of $\mathbf{B}_{i_n}^{(n)} (\in \mathbb{R}^{C \times C})$ is

$$\sum_{(i_1, \dots, i_N) \in \Omega_{i_n}^{(n)}} \left(\prod_{l \neq n} a_{i_l k_{c_1}}^{(l)} \prod_{l \neq n} a_{i_l k_{c_2}}^{(l)} \right),$$

the c th entry of $\mathbf{c}_{i_n}^{(n)} (\in \mathbb{R}^C)$ is

$$\sum_{(i_1, \dots, i_N) \in \Omega_{i_n}^{(n)}} \left(\hat{r}_{i_1 \dots i_N} \prod_{l \neq n} a_{i_l k_c}^{(l)} \right),$$

and \mathbf{I}_C is a C by C identity matrix. $\Omega_{i_n}^{(n)}$ denotes the subset of Ω whose n th mode's index is equal to i_n . The proof of this update rule is as follows:

Theorem 1:

$$\arg \min_{[a_{i_n k_1}^{(n)}, \dots, a_{i_n k_C}^{(n)}]^T} L(\mathbf{A}^{(1)}, \dots, \mathbf{A}^{(N)}) = (\mathbf{B}_{i_n}^{(n)} + \lambda \mathbf{I}_C)^{-1} \mathbf{c}_{i_n}^{(n)}$$

Proof:

$$\begin{aligned} \frac{\partial L}{\partial a_{i_n k_c}^{(n)}} &= 0, \forall c, 1 \leq c \leq C \\ \Leftrightarrow \sum_{(i_1, \dots, i_N) \in \Omega_{i_n}^{(n)}} \left(\left(\sum_{s=1}^C \prod_{l=1}^N a_{i_l k_s}^{(l)} - \hat{r}_{i_1 \dots i_N} \right) \prod_{l \neq n} a_{i_l k_c}^{(l)} \right) + \lambda a_{i_n k_c}^{(n)} &= 0, \forall c \\ \Leftrightarrow \sum_{(i_1, \dots, i_N) \in \Omega_{i_n}^{(n)}} \left(\sum_{s=1}^C \left(a_{i_n k_s}^{(n)} \prod_{l \neq n} a_{i_l k_s}^{(l)} \right) \prod_{l \neq n} a_{i_l k_c}^{(l)} \right) + \lambda a_{i_n k_c}^{(n)} &= 0 \\ = \sum_{(i_1, \dots, i_N) \in \Omega_{i_n}^{(n)}} \left(\hat{r}_{i_1 \dots i_N} \prod_{l \neq n} a_{i_l k_c}^{(l)} \right), \forall c & \\ \Leftrightarrow (\mathbf{B}_{i_n}^{(n)} + \lambda \mathbf{I}_C) [a_{i_n k_1}^{(n)}, \dots, a_{i_n k_C}^{(n)}]^T = \mathbf{c}_{i_n}^{(n)} & \end{aligned}$$

Since $\mathbf{B}_{i_n}^{(n)}$ is symmetric, Cholesky decomposition can be used for its inversion. After this rank C factorization, the entries of \mathcal{R} are updated by the following rule (line 1):

$$r_{i_1 \dots i_N} \leftarrow \hat{r}_{i_1 \dots i_N} - \sum_{c=1}^C \prod_{n=1}^N a_{i_n k_c}^{(n)}. \quad (5)$$

In CDTF, instead of computing $\hat{\mathcal{R}}$ before rank one factorization, containing the computation in (4) and (5) results in better performance on a disk-based system like MAPREDUCE by significantly reducing disk I/O operations. Moreover, updating columns in a fixed order instead of choosing them randomly converges faster in CDTF in our experiments.

B. Complexity Analysis

Theorem 2: The computational complexity of Algorithm 1 is $O(T_{out} |\Omega| N T_{in} K (N + C) + T_{out} T_{in} K C^2 \sum_{n=1}^N I_n)$.

Proof:

Computing $\hat{\mathbf{R}}$ (line 1) and updating \mathbf{R} (line 1) take $O(|\Omega|NC)$. Updating C parameters (line 1) takes $O(|\Omega_{i_n}^{(n)}|C(C+N)+C^3)$, which consists of $O(|\Omega_{i_n}^{(n)}|NC)$ to calculate $\prod_{l \neq n} a_{i_l k_1}^{(l)}$ through $\prod_{l \neq n} a_{i_l k_C}^{(l)}$ for all the entries in $|\Omega_{i_n}^{(n)}|$, $O(|\Omega_{i_n}^{(n)}|C^2)$ to build $\mathbf{B}_{i_n}^{(n)}$, $O(|\Omega_{i_n}^{(n)}|C)$ to build $\mathbf{c}_{i_n}^{(n)}$, and $O(C^3)$ to invert $\mathbf{B}_{i_n}^{(n)}$. Thus, updating all the entries in C columns (lines 1 through 1) takes $O(|\Omega|C(C+N)+I_n C^3)$, and the rank C factorization (lines 1 through 1) takes $O(|\Omega|NC(N+C)+C^3 \sum_{n=1}^N I_n)$. As a result, an outer iteration, which repeats the rank C factorization $T_{in}K/C$ times and both $\hat{\mathbf{R}}$ computation and \mathbf{R} update K/C times, takes $O(|\Omega|NT_{in}K(N+C)+T_{in}KC^2 \sum_{n=1}^N I_n)+O(|\Omega|NK)$, where the second term is dominated. ■

Theorem 3: The memory requirement of Algorithm 1 is $O(C \sum_{n=1}^N I_n)$.

Proof:

Since $\hat{\mathbf{R}}$ computation (line 1), rank C factorization (lines 1 through 1), and \mathbf{R} update (line 1) all depend only on the C columns of the factor matrices, the number of whose entries is $C \sum_{n=1}^N I_n$, the other $(K-C)$ columns do not need to be loaded into memory. Thus, the columns of the factor matrices can be loaded by turns depending on (k_1, \dots, k_C) values. Moreover, updating C columns (lines 1 through 1) can be processed by streaming the entries of $\hat{\mathbf{R}}$ from disk and processing them one by one instead of loading them all at once because the entries of $\mathbf{B}_{i_n}^{(n)}$ and $\mathbf{c}_{i_n}^{(n)}$ in the update rule are the sum of the values calculated independently from each $\hat{\mathbf{R}}$ entry. Likewise, $\hat{\mathbf{R}}$ computation and \mathbf{R} update can also be processed by streaming \mathbf{R} and $\hat{\mathbf{R}}$, respectively. ■

C. Parallelization in Distributed Environments

In this section, we describe how to parallelize SALS in distributed environments such as MAPREDUCE where machines do not share memory. Algorithm 2 depicts the distributed version of SALS.

Since update rule (4) for each row (C parameters) of a factor matrix does not depend on the other rows in the matrix, rows in a factor matrix can be distributed across machines and updated simultaneously without affecting the correctness of SALS. Each machine m updates mS_n rows of $\mathbf{A}^{(n)}$ (line 2), and for this, the $m\Omega = \bigcup_{n=1}^N \left(\bigcup_{i_n \in mS_n} \Omega_{i_n}^{(n)} \right)$ entries of \mathbf{X} are distributed to machine m in the first stage of the algorithm (line 2). Figure 2 shows an example of work and data distribution in SALS.

After the update, parameters updated by each machine are broadcasted to all other machines (line 2). Each machine m broadcasts $C|mS_n|$ parameters and receives $C(I_n - |mS_n|)$ parameters from the other machines after each update. The total number of parameters each machine exchanges with the other machines is $KT_{in} \sum_{n=1}^N I_n$ per outer iteration.

Algorithm 2: Distributed version of SALS

Input : \mathbf{X} , K , λ , mS_n for all m and n
Output: $\mathbf{A}^{(n)}$ for all n

```

1 distribute the  $m\Omega$  entries of  $\mathbf{X}$  to each machine  $m$ 
2 Parallel (P): initialize the  $m\Omega$  entries of  $\mathbf{R}$ 
3 P: initialize  $\mathbf{A}^{(n)}$  for all  $n$ 
4 for outer iter = 1.. $T_{out}$  do
5   for split iter = 1.. $\lceil \frac{K}{C} \rceil$  do
6     choose  $k_1, \dots, k_C$  (from columns not updated yet)
7     P: compute  $m\Omega$  entries of  $\hat{\mathbf{R}}$ 
8     for inner iter = 1.. $T_{in}$  do
9       for  $n = 1..N$  do
10        P: update  $\{a_{i_n k_c}^{(n)} | i_n \in mS_n, 1 \leq c \leq C\}$ 
11        using (4)
12        P: broadcast  $\{a_{i_n k_c}^{(n)} | i_n \in mS_n, 1 \leq c \leq C\}$ 
13      P: update the  $m\Omega$  entries of  $\mathbf{R}$  using (5)

```

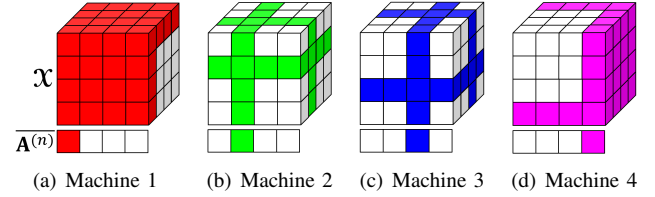


Figure 2: Work and data distribution of SALS in distributed environments with a 3-dimensional tensor and 4 machines. We assume that the rows of the factor matrices are assigned to the machines sequentially. The colored region of $\mathbf{A}^{(n)}$ (the transpose of $\mathbf{A}^{(n)}$) in each sub-figure corresponds to the parameters updated by each machine, resp., and that of \mathbf{X} corresponds to the data distributed to each machine.

The running time of parallel steps in Algorithm 2 depends on the longest running time among all machines. Specifically, the running time of lines 2, 2, and 2 is proportional to $\max_m |m\Omega^{(n)}|$ where $m\Omega^{(n)} = \bigcup_{i_n \in mS_n} \Omega_{i_n}^{(n)}$, and that of line 2 is proportional to $\max_m |mS_n|$. Therefore, it is necessary to assign the rows of the factor matrices to the machines (i.e., to decide mS_n) so that $|m\Omega^{(n)}|$ and $|mS_n|$ are even among all the machines. The greedy assignment algorithm described in Algorithm 3 aims to minimize $\max_m |m\Omega^{(n)}|$ under the condition that $\max_m |mS_n|$ is minimized (i.e., $|mS_n| = I_n/M$ for all n where M is the number of machines). For each factor matrix $\mathbf{A}^{(n)}$, we sort its rows in the decreasing order of $|\Omega_{i_n}^{(n)}|$ and assign the rows one by one to the machine m which satisfies $|mS_n| < \lceil I_n/M \rceil$ and has the smallest $|m\Omega^{(n)}|$ currently. The effects of this greedy row assignment on actual running times are described in Section V-E.

IV. OPTIMIZATION ON MAPREDUCE

In this section, we describe two optimization techniques used to implement SALS and CDTF on MAPREDUCE, which is one of the most widely used distributed platforms.

Algorithm 3: Greedy row assignment in SALS

Input : \mathcal{X}, M
Output: $_m S_n$ for all m and n

```
1 initialize  $|_m \Omega|$  to 0 for all  $m$ 
2 for  $n = 1..N$  do
3   initialize  $_m S_n$  to  $\emptyset$  for all  $m$ 
4   initialize  $|_m \Omega^{(n)}|$  to 0 for all  $m$ 
5   calculate  $|\Omega_{i_n}^{(n)}|$  for all  $i_n$ 
6   foreach  $i_n$  (in decreasing order of  $|\Omega_{i_n}^{(n)}|$ ) do
7     find  $m$  with  $|_m S_n| < \lceil \frac{I_n}{M} \rceil$  and the smallest  $|_m \Omega^{(n)}|$ 
8     (in case of a tie, choose the machine with smaller  $|_m S_n|$ ,
9     and if still a tie, choose the one with smaller  $|_m \Omega|$ )
10    add  $i_n$  to  $_m S_n$ 
11    add  $|\Omega_{i_n}^{(n)}|$  to  $|_m \Omega^{(n)}|$  and  $|_m \Omega|$ 
```

Algorithm 4: Parameter update in SALS without local disk caching

Given : n, k_c for all c , $_m S_n$ for all m , $\mathbf{a}_{*k_c}^{(l)}$ for all l and c
Input : $\hat{\mathcal{R}}$
Output: updated $\mathbf{a}_{*k_c}^{(n)}$ for all c

```
1 Map(Key k, Value v)
2 begin
3    $((i_1, \dots, i_N), \hat{r}_{i_1 \dots i_N}) \leftarrow v$ 
4   find  $m$  where  $i_n \in _m S_n$ 
5   emit  $\langle (m, i_n), ((i_1, \dots, i_N), \hat{r}_{i_1 \dots i_N}) \rangle$ 
6 end
7 Partitioner(Key k, Value v)
8 begin
9    $(m, i_n) \leftarrow k$ 
10  assign  $\langle k, v \rangle$  to machine  $m$ 
11 end
12 Reduce(Key k, Value v[1..r])
13 begin
14    $(m, i_n) \leftarrow k$ 
15    $\Omega_{i_n}^{(n)}$  entries of  $\hat{\mathcal{R}} \leftarrow v$ 
16   update and emit  $\mathbf{a}_{i_n k_c}^{(n)}$  for all  $c$ 
17 end
```

A. Local Disk Caching

Typical MAPREDUCE implementations of SALS and CDTF without local disk caching run each parallel step as a separate MAPREDUCE job. Algorithms 4 and 5 describe the MAPREDUCE implementations of parameter update (update of $\mathbf{a}_{*k_c}^{(n)}$ for all c) and \mathcal{R} update, respectively. $\hat{\mathcal{R}}$ computation can be implemented by the similar way with \mathcal{R} update, and broadcasting updated parameters is not necessary in this implementation because reducers terminate after updating their assigned parameters. Instead, the updated parameters are saved in the distributed file system and are read at the next step (a separate job). Since SALS repeats both \mathcal{R} update and $\hat{\mathcal{R}}$ computation $T_{in}K/C$ times and parameter update $KT_{in}N/C$ times at every outer iteration, this implementation repeats distributing \mathcal{R} or $\hat{\mathcal{R}}$ across machines (the mapper stage of Algorithms 4 and 5) $T_{out}K(T_{in}N + 2)/C$

Algorithm 5: \mathcal{R} update in SALS without local disk caching

Given : k_c for all c , $_m S_1$ for all m , $\mathbf{a}_{*k_c}^{(l)}$ for all l and c
Input : $\hat{\mathcal{R}}$
Output: updated \mathcal{R}

```
1 Map(Key k, Value v)
2 begin
3    $((i_1, \dots, i_N), \hat{r}_{i_1 \dots i_N}) \leftarrow v$ 
4   find  $m$  where  $i_1 \in _m S_1$ 
5   emit  $\langle m, ((i_1, \dots, i_N), \hat{r}_{i_1 \dots i_N}) \rangle$ 
6 end
7 Partitioner(Key k, Value v)
8 begin
9    $m \leftarrow k$ 
10  assign  $\langle k, v \rangle$  to machine  $m$ 
11 end
12 Reduce(Key k, Value v[1..r])
13 begin
14   foreach  $((i_1, \dots, i_N), \hat{r}_{i_1 \dots i_N}) \in v[1..r]$  do
15     update  $r_{i_1 \dots i_N}$ 
16     emit  $((i_1, \dots, i_N), r_{i_1 \dots i_N})$ 
17 end
```

Algorithm 6: Data distribution in SALS with local disk caching

Input : $\mathcal{X}, _m S_n$ for all m and n
Output: $_m \Omega^{(n)}$ entries of $\mathcal{R}(=\mathcal{X})$ for all m and n

```
1 Map(Key k, Value v);
2 begin
3    $((i_1, \dots, i_N), x_{i_1 \dots i_N}) \leftarrow v$ 
4   for  $n = 1, \dots, N$  do
5     find  $m$  where  $i_n \in _m S_n$ 
6     emit  $\langle (m, n), ((i_1, \dots, i_N), x_{i_1 \dots i_N}) \rangle$ 
7   end
8 Partitioner(Key k, Value v);
9 begin
10   $(m, n) \leftarrow k$ 
11  assign  $\langle k, v \rangle$  to machine  $m$ 
12 end
13 Reduce(Key k, Value v[1..r]);
14 begin
15    $(m, n) \leftarrow k$ 
16   open a file on the local disk to cache  $_m \Omega^{(n)}$  entries of  $\mathcal{R}$ 
17   foreach  $((i_1, \dots, i_N), x_{i_1 \dots i_N}) \in v[1..r]$  do
18     write  $((i_1, \dots, i_N), x_{i_1 \dots i_N})$  to the file
19 end
```

times, which is inefficient.

Our implementation reduces this inefficiency by caching data to local disk once they are distributed. In the SALS implementation with local disk caching, \mathcal{X} entries are distributed across machines and cached in the local disk during the map and reduce stage (Algorithm 6); and the rest part of SALS runs in the close stage (cleanup stage in Hadoop) using cached data. Our implementation streams the cached data, $_m \Omega^{(n)}$ entries of \mathcal{R} for example, from the local disk instead of distributing entire \mathcal{R} from the distributed file

Algorithm 7: Parameter broadcast in SALS

Input : $m\mathbf{a}_{*k_c}^{(n)}$ for all c (parameters to broadcast)
Output: $\mathbf{a}_{*k_c}^{(n)}, \forall c$ (parameters received from others)

```

1 begin
2   create a data file  $mA$  on the distributed file system (DFS)
3   write  $m\mathbf{a}_{*k_c}^{(n)}$  on the datafile
4   create a dummy file  $mD$  on DFS
5   while not all data files are read do
6     get the list of dummy files from DFS
7     foreach  $m'D$  in the list do
8       if  $m'A$  are not read then
9         read  $m'\mathbf{a}_{*k_c}^{(n)}$  from  $m'A$ 
10 end

```

system when updating the columns of $\mathbf{A}^{(n)}$. The effect of this local disk caching on actual running time is described in Section V-E.

B. Direct Communication

In MAPREDUCE, it is generally assumed that reducers run independently and do not communicate directly with each other. However, we adapt the direct communication method using the distributed file system in [1] to broadcast parameters among reducers efficiently. The implementation of parameter broadcast (broadcast of $\mathbf{a}_{*k_c}^{(n)}$ for all c) in SALS based on this method is described in Algorithm 7 where $m\mathbf{a}_{*k_c}^{(n)}$ denotes $\{a_{i_n k_c}^{(n)} | i_n \in mS_n\}$.

V. EXPERIMENTS

To evaluate SALS and CDTF, we design and conduct experiments to answer the following questions:

- **Q1: Data scalability (Section V-B).** How do CDTF, SALS, and other methods scale with regard to the following properties of an input tensor: dimension, the number of observations, mode length, and rank?
- **Q2: Machine scalability (Section V-C).** How do CDTF, SALS, and other methods scale with regard to the number of machines?
- **Q3: Convergence (Section V-D).** How quickly and accurately do CDTF, SALS, and other methods factorize real-world tensors?
- **Q4: Optimization (Section V-E).** How much do local disk caching and greedy row assignment improve the speed of SALS and CDTF? Can these optimization techniques be applied to other methods?
- **Q5: Effects of T_{in} (Section V-F)** How do different numbers of inner iterations (T_{in}) affect the convergence of CDTF?
- **Q6: Effects of C (Section V-G)** How do different numbers of columns updated at a time (C) affect the convergence of SALS?

Other methods include ALS, FLEXIFACT, and PSGD. All experiments are focused on the distributed version of each

Table IV: Summary of real-world datasets.

	MovieLens ₄	Netflix ₃	Yahoo-music ₄
N	4	3	4
I_1	715,670	2,649,429	1,000,990
I_2	65,133	17,770	624,961
I_3	169	74	133
I_4	24	-	24
$ \Omega $	93,012,740	99,072,112	252,800,275
$ \Omega _{test}$	6,987,800	1,408,395	4,003,960
K	20	40	80
λ	0.01	0.02	1.0
η_0	0.01	0.01	10^{-5} (FLEXIFACT) 10^{-4} (PSGD)

Table V: Scale of synthetic datasets. B: billion, M: million, K: thousand. The length of every mode is equal to I .

	S1	S2 (default)	S3	S4
N	2	3	4	5
I	300K	1M	3M	10M
$ \Omega $	30M	100M	300M	1B
K	30	100	300	1K

method, which is the most suitable to achieve our purpose of handling large-scale data.

A. Experimental Settings

1) **Cluster:** We run experiments on a 40-node Hadoop cluster. Each node has an Intel Xeon E5620 2.4GHz CPU. The maximum heap memory size per reducer is set to 8GB.

2) **Data:** We use both real-world and synthetic datasets most of which are available at <http://kdm.kaist.ac.kr/sals>. The real-world tensor data used in our experiments are summarized in Table IV with the following details:

- **MovieLens₄¹:** Movie rating data from MovieLens, an online movie recommender service. We convert them into a four-dimensional tensor where the third mode and the fourth mode correspond to (year, month) and hour-of-day when the movie is rated, respectively. The rates range from 1 to 5.
- **Netflix₃²:** Movie rating data used in Netflix prize. We regard them as a three-dimensional tensor where the third mode corresponds to (year, month) when the movie is rated. The rates range from 1 to 5.
- **Yahoo-music₄³:** Music rating data used in KDD CUP 2011. We convert them into a four-dimensional tensor by the same way in MovieLens₄. Since exact year and month are not provided, we use the values obtained by dividing the provided data (the number of days passed from an unrevealed date) with 30. The rates range from 0 to 100.

For reproducibility, we use the original training/test split offered by the data providers. Synthetic tensors are created by the procedure used in [10] to create Jumbo dataset. The scales of the synthetic datasets used are summarized in Table V.

¹<http://grouplens.org/datasets/movielens>

²<http://www.netflixprize.com>

³<http://webscope.sandbox.yahoo.com/catalog.php?datatype=c>

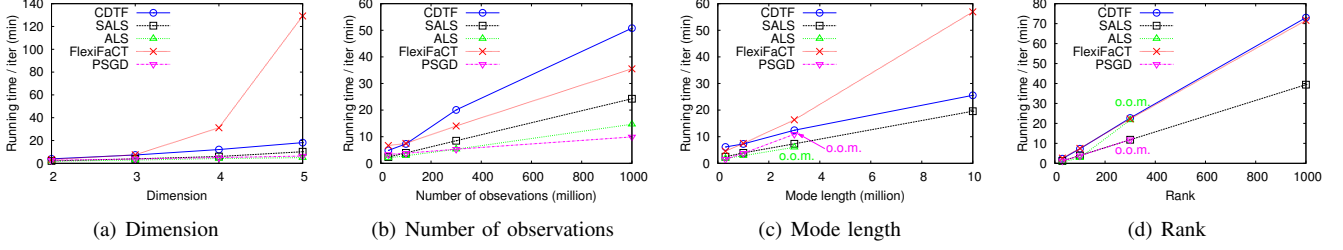


Figure 3: Scalability with regard to each aspect of data. o.o.m. : out of memory. Only SALS and CDTF scale with all the aspects.

3) *Implementation and Parameter Settings:* All methods in Table II are implemented using Java with Hadoop 1.0.3. Local disk caching, direct communication, and greedy row assignment are applied to all the methods if possible. All our implementations use weighted- λ -regularization [14]. For SALS and CDTF, T_{in} is set to 1, and C is set to 10, unless otherwise stated. The learning rate of FLEXIFACT and PSGD at t th iteration is set to $2\eta_0/(1+t)$, which follows the open-sourced FLEXIFACT implementation (<http://alexbeutel.com/l/flexifact/>). The number of reducers is set to 5 for FLEXIFACT, 20 for PSGD, and 40 for the other methods, each of which leads to the best performance on the machine scalability test in Section V-C, unless otherwise stated.

B. Data Scalability

1) *Scalability with Each Factor (Figure 3):* We measure the scalability of CDTF, SALS, and the competitors with regard to the dimension, number of observations, mode length, and rank of an input tensor. When measuring the scalability with regard to a factor, the factor is scaled up from S1 to S4 while all other factors are fixed at S2 as summarized in Table V. As seen in Figure 3(a), FLEXIFACT does not scale with dimension because of its communication cost, which increases exponentially with dimension. ALS and PSGD are not scalable with mode length and rank due to their high memory requirements as Figures 3(c) and 3(d) show. They require up to 11.2GB, which is $48\times$ of 234MB that CDTF requires and $10\times$ of 1,147MB that SALS requires. Moreover, the running time of ALS increases rapidly with rank owing to its cubically increasing computational cost. Only SALS and CDTF are scalable with all the factors as summarized in Table I. Their running times increase linearly with all the factors except dimension, with which they increase slightly faster due to the quadratically increasing computational cost.

2) *Overall Scalability (Figure 4(a)):* We measure the scalability of the methods by scaling up all the factors together from S1 to S4. The scalability of ALS and PSGD, and FLEXIFACT with 5 machines is limited owing to their high memory requirements. ALS and PSGD require almost 186GB to handle S4, which is $493\times$ of 387MB that CDTF requires and $100\times$ of 1,912MB that SALS requires. FLEXIFACT with 40 machines does not scale over S2 due to

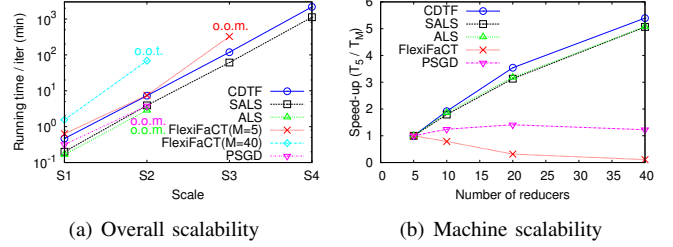


Figure 4: (a) Overall scalability. o.o.m. : out of memory, o.o.t. : out of time (takes more than a week). Only SALS and CDTF scale up to the largest scale S4. (b) Machine scalability. Computations of SALS and CDTF are efficiently distributed across machines.

its rapidly increasing communication cost. Only SALS and CDTF scale up to S4, and there is a trade-off between them: SALS runs faster, and CDTF is more memory-efficient.

C. Machine Scalability (Figure 4(b))

We measure the speed-ups (T_5/T_M where T_M is the running time with M reducers) of the methods on the S2 scale dataset by increasing the number of reducers. The speed-ups of CDTF, SALS, and ALS increase linearly at the beginning and then flatten out slowly owing to their fixed communication cost which does not depend on the number of reducers. The speed-up of PSGD flattens out fast, and PSGD even slightly slows down in 40 reducers because of increased overhead. FLEXIFACT slows down as the number of reducers increases because of its rapidly increasing communication cost.

D. Convergence (Figure 5)

We compare how quickly and accurately each method factorizes real-world tensors. Accuracies are calculated at each iteration by root mean square error (RMSE) on a held-out test set, which is a measure commonly used by recommendation systems. Table IV describes K , λ , and η_0 values used for each dataset. They are determined by cross validation. Owing to the non-convexity of (1), each algorithm may converge to local minima with different accuracies. In all datasets (results on the Movielens₄ dataset are omitted for space reasons), SALS is comparable with ALS, which converges the fastest to the best solution, and CDTF follows them. PSGD converges the slowest to the worst solution due to the non-identifiability of (1) [4].

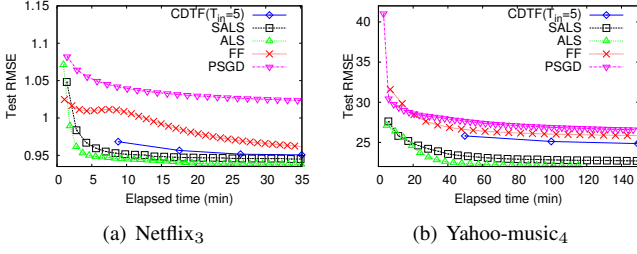


Figure 5: Convergence speed on real-world datasets. SALS is comparable with ALS, which converges fastest to the best solution, and CDTF follows them.

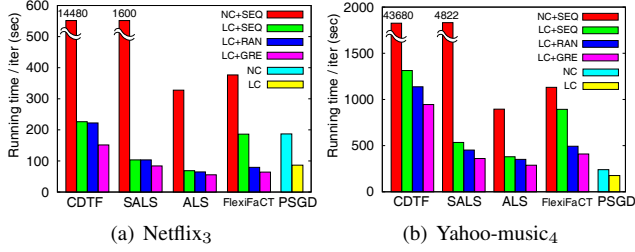


Figure 6: Effects of optimization techniques on running times. NC: no caching, LC: local disk caching, SEQ: sequential row assignment⁴, RAN: random row assignment, GRE: greedy row assignment. Our proposed optimization techniques (LC+GRE) significantly accelerate CDTF, SALS, and also their competitors.

E. Optimization (Figure 6)

We measure how our proposed optimization techniques, local disk caching and greedy row assignment, affect the running time of CDTF, SALS, and the competitors on real-world datasets. The direct communication method explained in Section IV-B is applied to all the implementations if necessary. Local disk caching speeds up CDTF up to $65.7\times$, SALS up to $15.5\times$, and the competitors up to $4.8\times$. The speed-ups of SALS and CDTF are the most significant because of the highly iterative nature of SALS and CDTF. Additionally, greedy row assignment speeds up CDTF up to $1.5\times$; SALS up to $1.3\times$; and the competitors up to $1.2\times$ compared with the second best one. It is not applicable to PSGD, which does not distribute parameters row by row.

F. Effects of Inner Iterations (T_{in})

Figure 7 compares the convergence properties of CDTF with different T_{in} values. As T_{in} increases, CDTF tends to converge more stably to better solutions (with lower test RMSE). However, there is an exception, $T_{in} = 1$ in the Netflix₃ dataset, which converges to the best solution.

G. Effects of the Number of Columns Updated at a Time (C)

The convergence properties of SALS with different C values are compared in Figure 8. T_{in} is fixed to 1 in all cases. As C increases, CDTF tends to converge faster to better

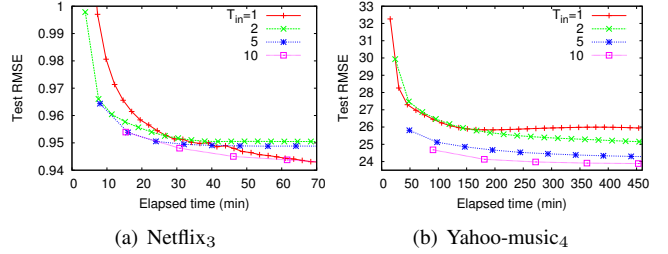


Figure 7: Effects of inner iterations (T_{in}) on the convergence of CDTF. CDTF tends to converge stably to better solutions as T_{in} increases.

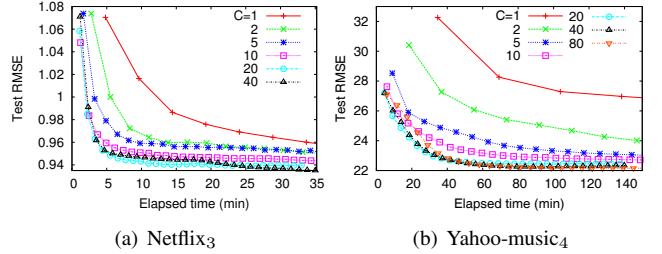


Figure 8: Effects of the number of columns updated at a time (C) on the convergence of SALS. SALS tends to converge faster to better solutions as C increases. However, its convergence speed decreases at C above 20.

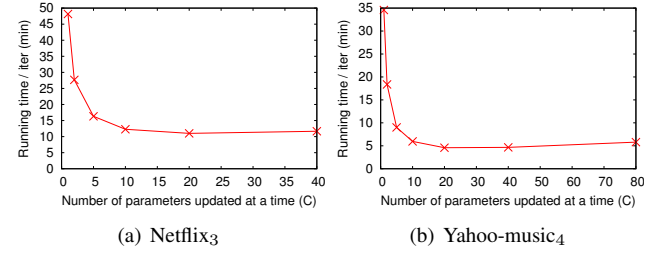


Figure 9: Effects of the number of columns updated at a time (C) on the running time of SALS. At low C values, running time per iteration decreases as C increases. However, this trend reverses at C greater than 20.

solutions (with lower test RMSE) although it requires more memory space as explained in the Theorem 3. With C above 20, however, convergence speed decreases as C increases. These changes in convergence speed are closely related to those in running time per iteration. As seen Figure 9, running time per iteration against C is a V-shaped curve with a minimum value at $C = 20$. As C increases, the amount of disk I/O declines since it depends on the number of times that the entries of \mathcal{R} are streamed from disk, which is inversely proportional to C . Conversely, computational cost increases quadratically with regard to C . At low C values, the decrease in the amount of disk I/O is greater and leads to a downward trend of running time per iteration. At high C values, however, the increase in the computational cost is greater and results in an upward trend of running time per iteration.

⁴ $mS_n = \{i_n \in \mathbb{N} | \frac{I_n \times (m-1)}{M} < i_n \leq \frac{I_n \times m}{M}\}$

VI. CONCLUSION

In this paper, we propose SALS and CDTF, distributed algorithms for high-dimensional and large-scale tensor factorization. They are scalable with all aspects of data (dimension, the number of observable entries, mode length, and rank) and show a trade-off: SALS has an advantage in terms of convergence speed, and CDTF has one in terms of memory usage. Local disk caching and greedy row assignment, two proposed optimization schemes, significantly accelerate not only SALS and CDTF but also their competitors.

ACKNOWLEDGMENTS

This work was supported by AFOSR/AOARD under the Grant No. FA2386-14-1-4036, and by the National Research Foundation of Korea (NRF) Grant funded by the Korean Government (MSIP) (No. 2013R1A1A1064409)

REFERENCES

- [1] A. Beutel, A. Kumar, E. E. Papalexakis, P. P. Talukdar, C. Faloutsos, and E. P. Xing. Flexifact: Scalable flexible factorization of coupled tensors on hadoop. In *SDM*, 2014.
- [2] P.-L. Chen, C.-T. Tsai, Y.-N. Chen, K.-C. Chou, C.-L. Li, C.-H. Tsai, K.-W. Wu, Y.-C. Chou, C.-Y. Li, W.-S. Lin, et al. A linear ensemble of individual and blended models for music rating prediction. *KDDCup 2011 Workshop*, 2011.
- [3] D. M. Dunlavy, T. G. Kolda, and E. Acar. Temporal link prediction using matrix and tensor factorizations. *ACM TKDD*, 5(2):10, 2011.
- [4] R. Gemulla, E. Nijkamp, P. Haas, and Y. Sismanis. Large-scale matrix factorization with distributed stochastic gradient descent. In *KDD*, 2011.
- [5] A. Karatzoglou, X. Amatriain, L. Baltrunas, and N. Oliver. Multiverse recommendation: N-dimensional tensor factorization for context-aware collaborative filtering. In *RecSys*, 2010.
- [6] T. Kolda and B. Bader. Tensor decompositions and applications. *SIAM review*, 51(3), 2009.
- [7] Y. Koren, R. Bell, and C. Volinsky. Matrix factorization techniques for recommender systems. *Computer*, 42(8):30–37, 2009.
- [8] R. McDonald, K. Hall, and G. Mann. Distributed training strategies for the structured perceptron. In *HLT-NAACL*, 2010.
- [9] A. Nanopoulos, D. Rafailidis, P. Symeonidis, and Y. Manolopoulos. Musicbox: Personalized music recommendation based on cubic analysis of social tags. *IEEE TASLP*, 18(2):407–412, 2010.
- [10] F. Niu, B. Recht, C. Ré, and S. J. Wright. Hogwild!: A lock-free approach to parallelizing stochastic gradient descent. *NIPS*, 2011.
- [11] J.-T. Sun, H.-J. Zeng, H. Liu, Y. Lu, and Z. Chen. Cubesvd: a novel approach to personalized web search. In *WWW*, 2005.
- [12] C.-J. H. S. S. Yu, Hsiang-Fu and I. S. Dhillon. Parallel matrix factorization for recommender systems. *Knowl. Inf. Syst.*, pages 1–27, 2013.
- [13] V. W. Zheng, B. Cao, Y. Zheng, X. Xie, and Q. Yang. Collaborative filtering meets mobile recommendation: A user-centered approach. In *AAAI*, 2010.
- [14] Y. Zhou, D. Wilkinson, R. Schreiber, and R. Pan. Large-scale parallel collaborative filtering for the netflix prize. In *AAIM*, pages 337–348. 2008.